



## **Classroom-ready open-source educational exoskeleton for biomedical and control engineering**

Downloaded from: <https://research.chalmers.se>, 2024-06-27 06:26 UTC

Citation for the original published paper (version of record):

Al-Tashi, M., Lennartson, B., Ortiz-Catalan, M. et al (2024). Classroom-ready open-source educational exoskeleton for biomedical and control engineering. *Automatisierungstechnik*, 72(5): 460-475. <http://dx.doi.org/10.1515/auto-2023-0208>

N.B. When citing this work, cite the original published paper.

## Tools

Mohammed Al-Tashi, Bengt Lennartson, Max Ortiz-Catalan and Fabian Just\*

# Classroom-ready open-source educational exoskeleton for biomedical and control engineering

Klassenraum-fertiges, selbst entwickelbares Exoskelett für Biomedizin- und Regelungstechnik

<https://doi.org/10.1515/auto-2023-0208>

Received November 20, 2023; accepted February 25, 2024

**Abstract:** In recent years, robotic arm exoskeletons have emerged as promising tools, finding widespread application in the rehabilitation of neurological disorders and as assistive devices for everyday activities, even alleviating the physical strain on labor-intensive tasks. Despite the growing prominence of exoskeletons in everyday life, a notable knowledge gap exists in the availability of open-source platforms for classroom-ready usage in educational settings. To address this deficiency, we introduce an open-source educational exoskeleton platform aimed at Science, Technology, Engineering, and Mathematics (STEM) education. This platform represents an enhancement of the commercial EduExo Pro by AUXIVO, tailored to serve as an educational resource for control engineering and biomedical engineering courses.

**Keywords:** educational exoskeleton; open-source; wearables; STEM; control engineering; biomedical engineering

**Zusammenfassung:** In den letzten Jahren haben sich robotische Exoskelette als vielversprechende Hilfsmittel herausgestellt, die breite Anwendung in der Rehabilitation neurologischer Erkrankungen und als allgemeine assistive Geräte für alltägliche Aktivitäten finden, indem sie beispielsweise die physische Belastung von arbeitsintensiven Aufgaben verringern. Trotz der wachsenden Bedeutung von Exoskeletten im täglichen Leben sind keine öffentlich zugänglichen Plattformen für die einsatzbereite Nutzung in Bildungseinrichtungen verfügbar. Um diese Lücke zu schließen, stellen wir eine öffentlich zugängliche, selbst entwickelbare Arm-Exoskelettplattform vor, die auf die Fächer Naturwissenschaften, Technologie, Ingenieurwesen und Mathematik (MINT) abzielt. Diese Plattform baut auf dem kommerziellen EduExo Pro von AUXIVO auf und ist darauf ausgerichtet, als Experimentierplattform für Kursinhalte im Bereich Regelungstechnik und Biomedizintechnik zu dienen.

**Schlagwörter:** Exoskelett; Regelungstechnik; Biomedizintechnik; Unterrichtsplattform; Open-Source; Experimentierplattform

\*Corresponding author: **Fabian Just**, Center of Bionics and Pain Research, Länsmansgatan 28, 431 30 Mölndal, Sweden; and Department of Electrical Engineering, Chalmers University of Technology, Chalmersplatsen 5, 42196, Gothenburg, Sweden, E-mail: [fabianjust@outlook.com](mailto:fabianjust@outlook.com).  
<https://orcid.org/0000-0002-9580-8189>

**Mohammed Al-Tashi**, Center of Bionics and Pain Research, Länsmansgatan 28, 431 30 Mölndal, Sweden,  
E-mail: [mohammedaltashi770@gmail.com](mailto:mohammedaltashi770@gmail.com)

**Bengt Lennartson**, Department of Electrical Engineering, Chalmers University of Technology, Chalmersplatsen 5, 42196, Gothenburg, Sweden,  
E-mail: [bengt.lennartson@chalmers.se](mailto:bengt.lennartson@chalmers.se)

**Max Ortiz-Catalan**, Center of Bionics and Pain Research, Länsmansgatan 28, 431 30 Mölndal, Sweden; Bionics Institute, 384-388 Albert St, East Melbourne, VIC 3002, Australia; and Medical Bionics Department, University of Melbourne, Parkville VIC 3052, Australia,  
E-mail: [maxortizc@outlook.com](mailto:maxortizc@outlook.com)

## 1 Introduction

In this era of rapid scientific and technological advancement, human-robot coexistence has become a reality [1]–[5]. Robots have found extensive applications across various domains of human life and production, with robotic exoskeletons emerging as a promising solution for movement impairment rehabilitation and physical performance enhancement [6]–[8]. Leveraging high-tech innovations, an

increasing number of robotic exoskeletons are designed to address these specific needs, utilizing advanced technologies to assist individuals with impaired mobility and enhance human performance in industries [9]–[11].

Simultaneously, the field of robotics has effectively engaged students in STEM education, and offers a hands-on and interactive approach to learning, allowing students to apply concepts from science, engineering, and math in a tangible and exciting way [12], [13]. By working with robots, students can develop critical thinking skills, problem-solving abilities, and creativity, all of which are essential for success in STEM disciplines [14]–[19]. Wearable robots, including robotic exoskeletons, have the potential to appeal to a wider audience by incorporating biological disciplines [20]–[22].

Additionally, STEM education has become a priority in multiple countries, as it develops critical abilities beyond technical disciplines [23]–[25]. Project-based robotics, especially for younger students, has shown potential as an effective educational tool [26]–[29]. Wearable robots, an emerging subfield within robotics, can increase interest in STEM due to their interface with biological systems [12], [21], [22], [25], [30], [31]. Robotic exoskeletons, in particular, have applications in healthcare and industry, making them appealing to less technically inclined students [32]–[36]. Creating educational tools for wearables, particularly robotic exoskeletons, can contribute to fostering at Science, Technology, Engineering, and Mathematics (STEM) interest and preparing students for the technology-driven future.

However, a significant challenge lies in the limited availability of open-source educational tools and readily accessible educational resources, which may present obstacles to their seamless integration into academic curricula within this domain [37]–[40]. This void is particularly conspicuous in the realm of biomedical studies, where the absence of adequate educational tools and projects is particularly striking [41], [42], despite their pronounced relevance to student learning and skill development. Furthermore, the limited time available to educational professionals for software development and resource creation presents a significant barrier [43], reinforcing the demand for pre-prepared, ready-to-use materials and tools.

In order to address this void, we introduce the Classroom Exo (Figure 1), an open-source educational robotic exoskeleton kit. This represents an enhanced iteration of the EduExo Pro, originally developed by the AUXIVO



**Figure 1:** The Classroom Exo on a mannequin: the Classroom Exo is a comprehensive arm exoskeleton covering the elbow to the shoulders, featuring a total of 3 degrees of freedom. A mechanical spring aids in lifting the shoulder joint, and a motor supports movement at the elbow joint. Additionally, the Classroom Exo is equipped with distinct charging and control ports, 2 EMG channels, a forearm force sensor, and an LED push button, offering visual feedback to the user.

team [44]. The Classroom Exo is meticulously designed to enhance usability for students and streamline the process of delivering practical courses encompassing a wide spectrum of subjects, including electronics, control engineering, software design, biomedical engineering, and scientific evaluation.

This paper presents a development framework for a robotic exoskeleton kit for educational purposes, targeted at a general audience with course applications from biomedical engineering to control engineering. We provided a detailed mechanical and electrical instruction manual and software including the graphical user interfaces for educators and students.<sup>1</sup> The work further aims to foster STEM education and exploration of wearable robot technologies by facilitating the way for others to contribute to the field.

## 2 Materials and methods

Recognizing the limitations of the EduExo Pro kit, particularly in terms of power source, maintenance, and usability within a classroom

<sup>1</sup> <https://github.com/fabianjust/classroom-exo>.



**Figure 2:** The EduExo Pro is an educational exoskeleton kit that contains hardware to assemble an arm exoskeleton (©Auxivo AG, Schwerzenbach, Switzerland).

environment, we placed a distinct emphasis on several key aspects. These include the seamless utilization of the exoskeleton, robust battery management systems, simplified maintenance procedures, an integrated error detection system, and an intuitively navigable graphical user interface.

## 2.1 EduExo Pro basis

The EduExo Pro is a comprehensive arm support system, spanning from the elbow to the shoulders. It consists of one active degree of freedom (elbow flexion/extension) and two passive degrees of freedom (horizontal shoulder abduction/adduction, shoulder elevation), providing a total of 3 degrees of freedom. EduExo Pro is sold by AUXIVO<sup>2</sup> and is the mechanical basis for our educational exoskeleton platform. Refer to Figure 2 for a visual representation of the EduExo Pro.

Additionally, the EduExo Pro kit has a handbook encompassing ten chapters, designed to provide an in-depth understanding of the current exoskeleton technology. However, it is imperative to highlight *Chapter 3: Anatomy and Mechanics*, as it is a guide through the process of assembling the mechanical and electrical components necessary for the basis of the Classroom Exo.

## 2.2 Upgrade of electrical system with a Printed Circuit Board (PCB)

We developed a PCB board to improve the EduExo Pro to be used in our classroom setting. We have enhanced several key aspects to optimize its performance and user experience. These improvements include:

- **Enhanced Power Supply:** We have transitioned from the original 6 AA battery power source utilized by the EduExo Pro to a more robust and efficient solution. Specifically, we replaced the conventional AA batteries with a 2-cell Li-Polymer (LiPo) battery. This modification ensures that the servo can operate at its maximum capacity, significantly bolstering the overall performance of the exoskeleton.

**Table 1:** Overview of components utilized in the PCB, including quantity and total pricing in euro.

Item	Quantity	Total price
Capacitor	18	€2.00
Diode	6	€2.00
Terminal block	5	€7.00
Inductor	1	€1.00
MOSFETs	2	€1.00
Resistor	15	€1.00
IC	1	€3.00
LED button	1	€10.00
Test point	19	€7.00
USB port	1	€1.00
Battery	1	€18.00

- **User-Friendly Battery Access:** The new design facilitates easy battery replacement, eliminating the need for users to open the electronic box of the exoskeleton, thus simplifying maintenance and operation.
- **Streamlined Circuitry:** The Classroom Exo design features conductive pathways, tracks, or signal traces etched from copper sheets laminated onto a non-conductive substrate. This reduces the complexity associated with manual wiring on a prototype circuit board. This simplification enhances the system’s reliability and ease of troubleshooting.
- **Enhanced Safety Measures:** In response to safety concerns, we have implemented a robust protection IC, the BQ25886, in the PCB. This advanced integrated circuit serves as a safeguard for the microcontroller and battery, offering overvoltage, over-current, and over-temperature protection. The BQ25886 effectively mitigates potential risks associated with errors or malfunctions, ensuring the reliable and secure operation of the exoskeleton.

These enhancements have been thoughtfully implemented to bolster the exoskeleton’s overall functionality and user experience. This PCB integrates a comprehensive solution, featuring an advanced protection system, a convenient USB port, and efficient battery management linked to a LIPO battery.

The Printed Circuit Board file is accessible as an open-source.<sup>3</sup> Please refer to Table 1 for detailed information on the components, including quantity and pricing.

## 2.3 USB port & LIPO battery

To enhance the power source usability within the exoskeleton, we have undertaken an innovative solution. We have transitioned from traditional AA batteries to a 2-cell Li-Polymer (LIPO) battery configuration, thereby significantly improving the power system. This upgrade not only provides a significant boost in power capacity but also enhances the overall performance of the EduExo Pro. Furthermore, we have incorporated a highly convenient and user-friendly feature by implementing a USB micro-B Connector. This ingenious addition

<sup>2</sup> [www.auxivo.com/products](http://www.auxivo.com/products).

<sup>3</sup> <https://github.com/fabianjust/classroom-exo/pcb>.

empowers users to effortlessly charge the Li-Polymer battery using a simple charging cable. With this streamlined process, users can easily recharge the Exoskeleton and ensure consistent and uninterrupted operation.

We have also introduced two visually informative indicators. Located near the USB micro-B Connector, two LEDs – one blue and one red – have been thoughtfully integrated. These LEDs serve as intuitive charge status indicators, offering clear visual cues to users about the ongoing charging process.

The blue LED provides detailed charge status information:

- HIGH indicates that the charging process is in progress.
- LOW indicates that the charge is complete or that charging is disabled.
- In the event of a fault, the blue LED pin blinks at 1 Hz.

On the other hand, the red LED is designed to indicate the quality of the input source:

- HIGH indicates a good input source.

With a mere glance, users can ascertain not only whether the exoskeleton is halfway or fully charged but also receive information about potential faults or the quality of the input source, enhancing their understanding and ensuring optimal usage.

## 2.4 BQ25886 integrated power management circuit

One of the standout features of the BQ25886, illustrated in Figure 3, is its ability to provide instant power activation, ensuring prompt availability of power whenever it is needed. This instantaneous response greatly enhances user experience and facilitates the seamless operation of devices powered by 2-cell Li-polymer batteries. The BQ25886, being an integrated circuit (IC), boasts precise termination control, enabling accurate monitoring and management of the charging process. This level of control not only enhances the battery's overall lifespan but also optimizes its performance and efficiency.

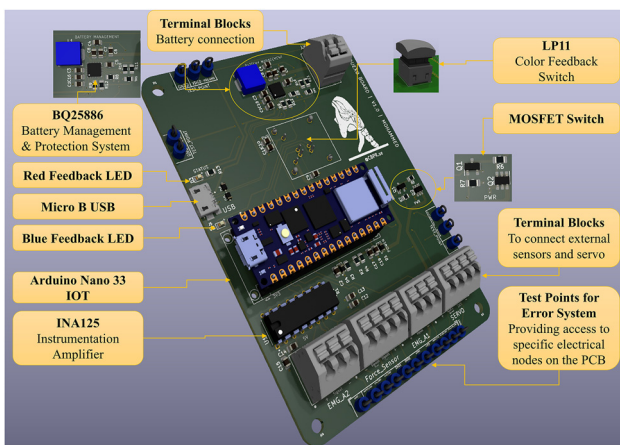


**Figure 3:** Printed Circuit Board (PCB) design for the Classroom Exo educational exoskeleton platform.

In addition to its impressive power management capabilities, the BQ25886 includes built-in protection circuits. These circuits play a vital role in safeguarding both the battery and any powered components from potential risks and hazards. By proactively detecting and mitigating potential issues, this integrated protection functions as a safety net, designed to intervene and mitigate the consequences of inadvertent exoskeleton misuse.

## 2.5 MOSFET switch

To give the user more control over the Exoskeleton, we have implemented a MOSFET switch to switch on and off the Servo through the microcontroller. This feature enables the user to control the power source of the servo, thereby providing greater flexibility and ease of use. Additionally, the user can use the sensors in the exoskeleton while the servo is off since it has its own implemented switch. This feature gives the user more usability and allows them to perform tasks that require sensor data without having to turn on the servo.

## 2.6 Microcontroller “Arduino Nano 33 IOT”

The core of the exoskeleton electronics is the microcontroller, a versatile component that not only acts as a miniature computer with integrated elements on a single board but also serves as a crucial software and programming device. The selected microcontroller for the EduExo Pro as well as for the Classroom Exo is the Arduino Nano 33 IOT. In addition to its hardware capabilities, this microcontroller plays a pivotal role in software-related functions, including reading signals from both position and force sensors. Moreover, it takes charge of programming tasks, controlling the intricate movements of the motor, and ensuring the seamless integration of hardware and software components within the exoskeleton system.

## 2.7 Software design and implementation

To initiate exoskeleton operation, the initial step involves the interconnection of its components. To enhance user interaction with the exoskeleton and ensure a user-friendly experience, a graphical user interface (GUI) was developed. Notably, MATLAB App Designer was chosen for the exoskeleton due to several compelling reasons. It boasts an open-source nature, possesses a vibrant and supportive community, offers an easily comprehensible platform for student modifications, and crucially, features robust serial communication libraries compatible with Arduino, a fundamental requirement. Additionally, MATLAB App Designer provides a repository of libraries and built-in functions. Furthermore, it grants the capacity to generate real-time graphical representations, which can be used to effectively present component and sensor values within the exoskeleton. The software was designed with a dual emphasis on two core domains, namely control systems and biomedical engineering.<sup>4</sup>

<sup>4</sup> <https://github.com/fabianjust/classroom-exo/controldevelopment>.

### 3 Enhanced position control with a tunable PID controller

The incorporation of a Proportional-Integral-Derivative (PID) control system within the realm of hobby servo position control represents a notable progression in the field of control systems. This application is specifically engineered to attain precise regulation and sustenance of the position of a hobby servo motor – an integral component employed across diverse domains, including robotics, automation, and model engineering.

The foundational mathematical expression underpinning any PID control implementation can be succinctly defined as follows:

$$u(t) = k_p e(t) + k_i \int_0^t e(\tau) d\tau + k_d \frac{de(t)}{dt} \quad (1)$$

wherein  $e(t)$  symbolizes the error term, and in the context of position control,  $x_{ref}(t)$  represents the set position while  $y(t)$  signifies the present position.

$$e(t) = x_{ref}(t) - y(t) \quad (2)$$

To facilitate a more intuitive grasp of the practical application of these mathematical principles within the servo motor domain, a visual representation is indispensable. Figure 4 elucidates the block diagram illustrating the PID control system for servo motors.

Key components featured in the system encompass a *Set Position* input, denoting the reference position for the actuator,  $x_{ref}(t)$ , a pulse-width-modulated (PWM) signal characterized by its duty cycle, which actuates the motor  $u(t)$ , and the *Current Position* of the actuator,  $y(t)$ .

This system is classified as a closed-loop control system, premised on the integration of a feedback loop. This mechanism relays real-time information concerning the prevailing

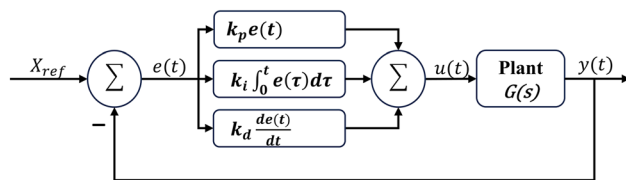


**Figure 4:** Servo PID control system with the reference elbow angle  $x_{ref}(t)$ , the current elbow angle  $y(t)$ , and the error  $e(t)$ .

state of the system, thereby enabling a continuous evaluation of the divergence between the current state and the desired setpoint.

In our specific application, the subtraction of the *Current Position* from the *Set Position* yields the Error signal  $e(t)$ , as depicted in (2).

The three control signals are subsequently derived from the Error signal and are generated by the Proportional, Integral, and Derivative blocks, each labeled with their respective gains,  $k_p$ ,  $k_i$ , and  $k_d$ . These control signals are subsequently combined to ascertain the Duty Cycle of the PWM signal, responsible for actuating the motor.

#### 3.1 Graphical user interface (GUI) for PID control

Based on the explanation above, we have devised a user-friendly graphical user interface (GUI) underpinned by a PID simulator. This GUI efficiently displays a comprehensive range of system responses generated by different input signal and control action combinations. Its versatile design also allows for the analysis of transfer functions. The displayed response output will be tested and compared with the output angle signal from the integrated position sensor in the servomotor.

The PID Graphical User Interface is composed of two main panels and a Graph described below:

- Transfer Function Panel.
- Exoskeleton Setting Panel.
- Step Response and Servo's Trajectory Graph.

**The Transfer Function Panel** facilitates the manipulation and fine-tuning of control system parameters. It consists of three sub-panels: Plant  $G(s)$ , Tuning PID, and Information Display.

The Plant  $G(s)$  sub-panel enables users to modify the transfer function parameters in the Laplace domain. Users can input coefficients for the numerator and denominator of the transfer function, allowing for frequency and time domain analyses.

The Tuning PID sub-panel allows customization of the proportional, integral, and derivative parameters of the PID controller. This feature empowers users to optimize the control system's response according to specific requirements.

The Information Display sub-panel provides insights into the system's behavior, showcasing Time Domain Specifications of a step response. Observe the Transfer Function Panel visually in Figure 5A for reference.

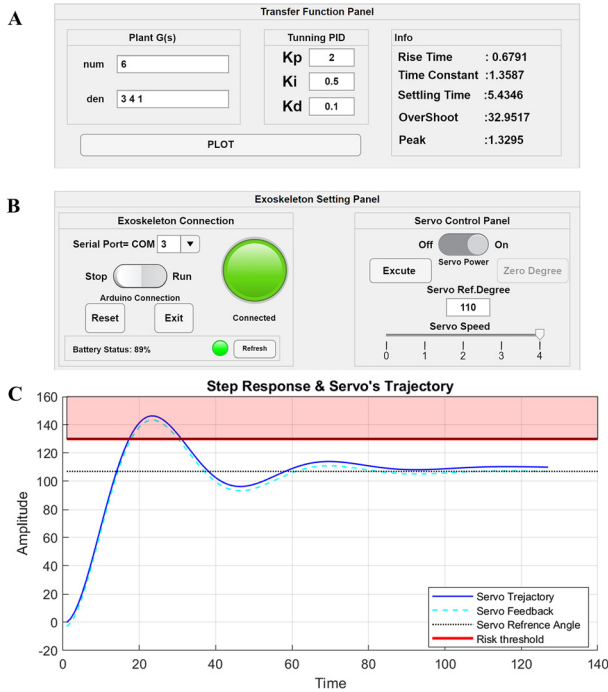


**Figure 5:** Graphical user interface (GUI) for PID control system on Classroom Exo educational platform showcasing: (A) transfer function panel for PID parameter tuning, (B) exoskeleton setting panel enabling connection to PC, and (C) graph displaying step response and servo Trajectory.

The **Exoskeleton Setting Panel** serves as an interface for connecting the user's PC to the Exoskeleton and controlling servo parameters. It comprises two sub-panels: Exoskeleton Connection and Servo Control.

The Exoskeleton Connection sub-panel enables users to select the COM port number and establish a connection with the Exoskeleton's microcontroller. Battery status information and informative warnings are also provided.

The Servo Control sub-panel offers control over the servomotor, allowing users to activate/deactivate the servo, initiate servo motion, and set reference angles. Refer to Figure 5B for a visual representation of the Exoskeleton Setting Panel.

The **Step Response and Servo Trajectory Graph** displays the expected step response of the control system and the servo trajectory. It features a Risk Threshold to ensure user safety and offers a practical comparison between simulated and actual servo responses. Examine Figure 5C for a graphical illustration of the Graph.

Overall, the PID controller GUI provides a user-friendly platform for configuring and analyzing control

systems, enhancing efficiency and performance for various applications.

## 4 Enhanced position control with a tunable PI controller

Continuing our exploration into position control, we shift our attention from the PID controller to its streamlined counterpart—the PI controller. This transition is deliberate, aligning with the widely recognized significance of PID controllers and setting the stage for a nuanced discussion on the PI controller's characteristics and tuning methodologies.

The PI controller, a prevalent variant, incorporates proportional (P) and integral (I) control actions to a suitable degree. Refer to Figure 6 for an overview of the feedback control system, incorporating a PI controller [45].

In industrial settings, the PI controller stands out as the most commonly used type. The transfer function for the *PI controller* ( $F_{PI}(s)$ ) is expressed as follows:

$$F_{PI}(s) = K_p \frac{1 + T_i s}{T_i s} \quad (3)$$

where,  $K_i$  = proportional gain.  $T_i$  = integral time constant.

The servo used in the Classroom Exo relies on traditional servo technology, responding to changes in the reference signal. To compensate for this, a *lag filter* with similar characteristics is employed, known as a lag filter with the transfer function ( $F_{lag}(s)$ ):

$$F_{lag}(s) = a \frac{1 + T_i s}{1 + a T_i s} = \frac{1 + T_i s}{\frac{1}{a} + T_i s} \quad \text{where } a > 1$$

The low-frequency gain of the lag filter is  $F_{lag}(0) = a$ . When we allow this gain, referred to as the lag ratio, to approach infinity, the lag filter can be simplified to:

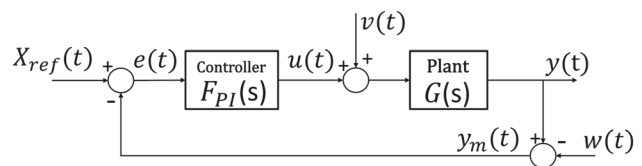


**Figure 6:** Feedback control system with PI controller; where  $G(s)$  is the general designation for the transfer function, as well as the process model from the control signal  $u(t)$  to the output signal  $y(t)$ ,  $F_{PI}(s)$  is the PI controller,  $X_{ref}(t)$  is the reference signal (setpoint),  $y_m(t)$  is the measured output signal of the process,  $v(t)$  is process disturbance, load disturbance, and  $w(t)$  is measurement disturbance.

$$F_{lag}(s) = \frac{1 + T_i s}{T_i s} \quad (4)$$

According to equation (3) and (4), the PI controller can be expressed using this lag filter:

$$F_{PI}(s) = K_p \cdot F_{lag}(s) = K_i \frac{1 + T_i s}{s} \quad (5)$$

When incorporating a PI controller in an industrial control system, the integral gain ( $K_i$ ) is often converted into the proportional gain  $K_p$  using the relationship  $K_p = K_i T_i$ . Both  $K_i$  and the integral gain  $T_i$  serve as user-adjustable setting parameters, allowing traditional control system users to influence the controller's behavior in practical applications.

#### 4.1 PI controller characteristics

The Bode diagram for the PI controller is depicted in Figure 6. The magnitude curve illustrates that, at low frequencies, the PI controller behaves akin to an I controller  $K_i/s$ .

While at higher frequencies, it functions as a P controller with the gain  $K_p = K_i T_i$ .

The low-frequency amplification  $K_i/s$ , tending towards infinity as  $\omega \rightarrow 0$ , serves to prevent residual errors in the presence of step disturbances and changes in the reference signal with step shapes.

However, this advantage in positive static properties comes at the expense of a significant negative phase shift  $\angle F_{PI}(j\omega) \approx -90^\circ$ , at small  $\omega$ . This substantial negative phase shift can pose stability challenges during feedback. Fortunately, the negative impact is counteracted by the proportional (P) effect at higher frequencies, resulting in a negligible phase shift  $\angle F_{PI}(s) \approx 0$ , as depicted in Figure 7.

The desirability of a high integral gain  $K_i$  becomes evident in terms of performance, especially in compensating for process disturbances  $J_v = 1/K_i$ . However, from a stability perspective, a smaller  $K_i$  is preferred to minimize the integral effect. Striking a balance between performance and stability involves establishing a critical requirement for robust stability margins while simultaneously maximizing  $K_i$ . These observations form the basis of the optimizing PI parameters using a phase margin  $\varphi_m$  and cross-frequency  $\omega_c$  which will be presented in the following subsections.

#### 4.2 Tuning PI controller utilizing phase margin $\varphi_m$ and crossover frequency $\omega_c$

Employing phase margin  $\varphi_m$  and crossover frequency  $\omega_c$  for tuning  $K_i$  and  $T_i$  in a PI controller facilitates a comprehensive understanding of the system's behavior, enabling

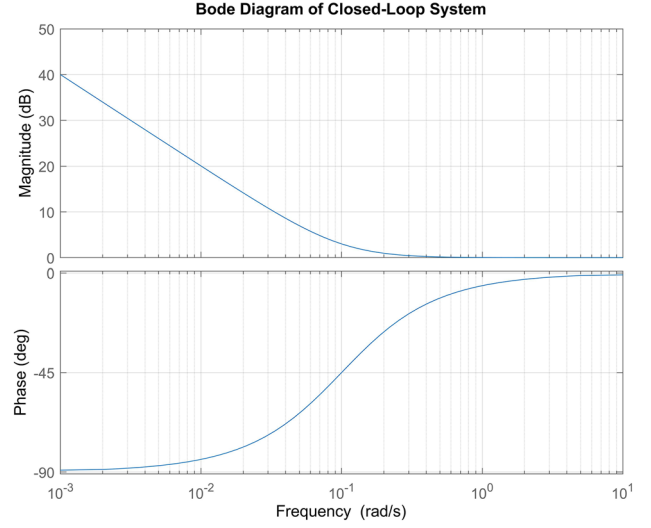


**Figure 7:** Bode diagram of the PI controller illustrating its dual behavior – acting as an I controller at low frequencies and as a P controller with increased gain at higher frequencies.

users to achieve a balance between stability and performance according to their requirements (increased  $\omega_c$  gives a faster feedback system).

The PI controller (5) at the crossover frequency  $\omega_c$  can be expressed as

$$F_{PI}(j\omega_c) = \frac{K_i}{\omega_c} (\omega_c T_i - j) \quad (6)$$

which means that the phase of the PI controller

$$\angle F_{PI}(j\omega_c) = -\arctan\left(\frac{1}{\omega_c T_i}\right) \quad (7)$$

We know that  $L(s)$  circuit feedback, in unit feedback  $L(s) = G(s)F(s)$ , where  $G(s)$  is the transfer function of the Plant and  $F(s)$  is the transfer function of the controller. Also,  $L(s)$  magnitude and phase margin at the cross frequency  $\omega_c$  can be represented as

$$|L(j\omega_c)| = 1 \ \& \ \angle L(j\omega_c) = -180^\circ + \varphi_m$$

which means that the phase of the PI controller can be expressed as

$$\angle F_{PI}(j\omega_c) = -180^\circ + \varphi_m - \angle G(j\omega_c) \quad (8)$$

According to (7), integral time constant  $T_i$  can be expressed as

$$T_i = \frac{1}{\omega_c} \cot(-\angle F_{PI}(j\omega_c)) \quad (9)$$



Since  $|L(j\omega_c)| = |G(j\omega_c)||F_{PI}(j\omega_c)|$  and according to (9), the Integral gain  $K_i$  can be represented as

$$K_i = \frac{\omega_c}{|G(j\omega_c)|\sqrt{1 + \cot^2(-\angle F_{PI}(j\omega_c))}} \quad (10)$$

After providing a comprehensive overview of the PI controller and its correlation with phase margin and crossover frequency, we now explore the practical implementation within our PI controller GUI.

### 4.3 Graphical user interface (GUI) for PI control

Our approach to Control PI Graphical User Interface involves two primary methods, catering to user preferences and ensuring optimal controller performance. *Method #1*, where users have direct control over key parameters, and *Method #2*, an automated optimization algorithm.

Before delving into the explanation of the two methods, let's provide a brief overview of the PI GUI structure. The PI GUI comprises two primary panels for control and connection:

- *G(s)* Plant & Tuning PI Controller Panel: this panel enables users to input the numerator and denominator values of the Plant's transfer function.
- Exoskeleton Setting Panel: this panel facilitates the connection between the user's device and the Classroom Exo.

Additionally, the GUI features three graphs:

- Reference Signal Graph: Displays the reference signal for the system.
- Disturbance Signal Graph: Illustrates the disturbance signal affecting the system.

The *G(s)* Plant Panel allows users to input the parameters of the Plant's transfer function, while the Tuning PI Controller Panel enables the adjustment of the phase margin  $\varphi_m$  and crossover frequency  $\omega_c$  to optimize performance. The panel includes a "Compare Changes" switch for graphical comparison of multiple parameter values. Moreover, it offers an "Optimize PI" button for automated tuning of  $\varphi_m$  and  $\omega_c$ .

In addition to these panels, a button is provided to plot the transfer function and PI controller equations. This feature allows users to visualize the Reference Signal and Disturbance Signal graphs of the Plant and PI controller configurations.

### 4.4 Using manual input for tuning: method #1

In this method, users directly input their preferred values for phase margin  $\varphi_m$  and crossover frequency  $\omega_c$ , offering a user-friendly interface. However, it is crucial to note that  $\omega_c$  should not be excessively high to achieve the desired  $\varphi_m$ . Studies suggest that setting  $\omega_c$  using the formula.

$$\omega_c = 0.4\omega_{G150} \quad (11)$$

yields nearly optimal outcomes, where  $\omega_{G150}$  is the frequency at which the process transfer function exhibits a phase shift of  $\angle G(j\omega_{G150}) = -150^\circ$ .

Procedure for Method #1

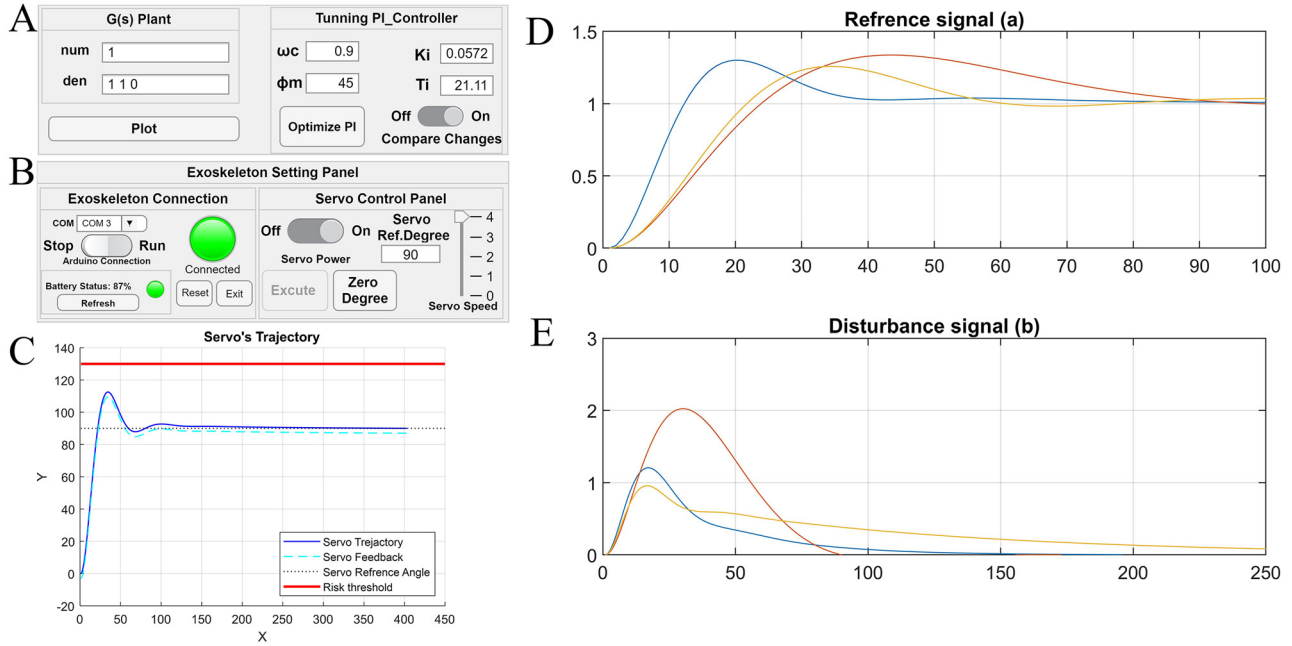
- Choose a suitable phase margin  $\varphi_m$  within the range of  $45^\circ - 60^\circ$  (e.g.,  $45^\circ$ ) and determine the crossover frequency  $\omega_c$  based on (11).
- Determine  $|G(j\omega_c)|$ ,  $\angle G(j\omega_c)$ , and consequently,  $\angle F_{PI}(j\omega_c)$  using Equation (8).
- Calculate  $T_i$  and  $K_i$  based on Equations (9) and (10).
- Utilize step plots to identify the optimal values  $T_i$  and  $K_i$ .

Figure 8 illustrate an example involving the control of a DC motor with a transfer function  $(s) = \frac{1}{s(1+s)}$ , employing a PI controller through our PI controller GUI. In this example, we explore the impact of varying phase margin and cross-frequency values, highlighting their influence on the resulting feedback system, as depicted in Figure 8D and E.

Additionally, the output of the feedback system is showcased in Figure 8 for different scenarios, where  $\varphi_m = 45^\circ$  is kept constant, and  $\omega_c$  is randomly set to 0.4, 0.7, and 0.9. Two distinct conditions are considered: (D) when the reference signal is a unit step and (E) when the disturbance signal is a unit step.

In particular, Figure 8E shows that it is disadvantageous both to choose too small a crossover frequency ( $\omega_c = 0.4$ ) and too large a value ( $\omega_c = 0.9$ ). Of the three cases, the middle value ( $\omega_c = 0.7$ ) gives the smallest area under  $y(t)$  in Figure 8E. Finally, it is observed that the above recommendation of  $\omega_c$  (11) in this example gives  $\omega_c = 0.4\omega_{G150} = 0.4 \times 1.73 = 0.69$ .

**Note for Comparison Analysis:** For users aiming to conduct a graphical comparison of multiple values for the phase margin or cross-frequency, it is recommended to activate the "Compare Changing" switch in the Tuning PI Controller Panel. Enabling this feature facilitates a comprehensive visual assessment of the system's response under



**Figure 8:** Illustration of the PI controller GUI regulating a DC motor with the transfer function  $G(s) = \frac{1}{s(1+s)}$ . (A)  $G(s)$  plant & tuning PI controller panel, (B) exoskeleton setting panel for PC connection, (C) graph depicting the Servo's trajectory, (D) step response from the reference signal to the output, and (E) step response from the disturbance signal to the output.

various parameter settings, aiding in effective tuning and analysis.

### 4.5 Auto optimization for PI parameters: method #2

The second method involves leveraging our optimization algorithms to automatically determine the optimal values for phase margin, crossover frequency,  $K_i$  (integral gain), and  $T_i$  (integral time constant). This automated approach ensures an optimal solution, enhancing controller performance with minimal user intervention.

This method entails a two-step procedure: first, it identifies the optimal values for the  $T_i$  and  $K_i$  parameters, and subsequently, it assesses the stability of the system.

Optimization with respect to  $T_i$  and  $K_i$  parameters: The earlier example emphasized the delicate balance required for choosing the crossover frequency  $\omega_c$  in a PI controller, highlighting the need for neither excessively large nor too small values to effectively address process disturbances. Consequently, the optimization algorithm aims to directly explore combinations of the controller parameters  $T_i$  and  $K_i$  that minimize the performance criterion  $J_v = \frac{1}{K_i}$ , while maintaining robust stability margins.

Given that the criterion ( $J_v$ ) to be minimized is the inverse of the controller parameter  $K_i$ , the optimization problem simplifies to finding the integral time constant  $T_i$

that maximizes  $K_i$ , subject to secondary conditions on the  $M_s$  (the maximum gain of the sensitivity function) and  $M_T$  (complementary sensitivity function maximum gain).

$$\max_{T_i} K_i \quad M_s \leq 1.7 \quad M_T \leq 1.3 \quad (12)$$

Solving this intricate nonlinear optimization problem typically involves iterative search methods. The selection of initial values for  $T_i$  and  $K_i$  is crucial, considering that many combinations might lead to an unstable feedback system. Determining suitable starting values is process-dependent, and establishing general rules is inherently challenging.

For numerous process models, optimal values for phase margin  $\phi_m$  and crossover frequency  $\omega_c$  often fall within the ranges:

$$45^\circ \leq \phi_m \leq 60^\circ \quad (13)$$

$$0.3\omega_{G150} \leq \omega_c \leq 0.5\omega_{G150} \quad (14)$$

In light of these observations, the reformulated optimization problem equation (12) now incorporates equations (13) and (14):

$$\max_{\phi_m, \omega_c} K_i \quad M_s \leq 1.7 \quad M_T \leq 1.3 \quad (15)$$

Following the determination of optimal values for the  $T_i$  and  $K_i$  parameters, the algorithm proceeds to assess the stability of the system. Stability verification is carried out by  $H_2$  norm.

### 4.6 H2 norm

The  $H_2$  norm measures the energy response of a system to an impulse input. In the context of control systems, it quantifies the energy gain of the closed-loop system, evaluating its ability to minimize disturbances and maintain stability.

$$\|G_2\| = \sqrt{\int_0^\infty g(t)^2 dt}$$

where  $g(t)$  is the impulse function response. The  $H_2$  norm provides a quantitative measure of the system’s stability. For control systems, a bounded  $H_2$  norm indicates that the system responds effectively to inputs while minimizing energy, ensuring stability. In the MATLAB code, stability is assessed by checking that the  $H_2$  norm is less than infinity.

It is essential to note that the entire procedure outlined in Method #2 is seamlessly executed by simply pressing the ‘Optimize PI’ button in the ‘Tunning PI Controller Panel’ after entering the plant transfer function  $G(s)$ . This automated process ensures a user-friendly experience and minimizes the need for extensive manual intervention.

Upon initiating the optimization, the algorithm automatically determines the optimal values for phase margin, crossover frequency,  $T_i$  and  $K_i$ . The ‘Optimize PI’ button serves as a convenient gateway to an efficient and effective tuning process, streamlining the complexities of controller optimization. This automated approach not only enhances user convenience but also ensures consistency and accuracy in obtaining optimal parameters for the PI controller.

## 5 Force control development

The force sensor plays a pivotal role in our exoskeleton system, serving a dual purpose of measuring interaction forces between the exoskeleton and the user while also functioning as a control input for exoskeleton operation.

To measure interaction forces accurately, we convert physical force (in Newtons, N) into an electric signal (in volts, V) using a force sensor. This sensor consists of a metal structure with strain gauges that change resistance in response to force. When force is applied, the strain gauges undergo minute deformations, altering their resistance. These resistors are interconnected in a Wheatstone bridge circuit for precise measurements of resistance variations. An amplifier chip magnifies the output voltage for interpretation by the microcontroller.

Understanding the force sensor’s operation, we designed a control system responsive to arm movements.

The sensor’s output voltage indicates force direction, allowing us to establish upper and lower thresholds. When values exceed the upper threshold, the servo moves upward, and vice versa. This synchronized system aligns servo movement with applied force duration.

To optimize force control, we applied a Digital Low Pass Filter to smooth force sensor values, enhancing precision and stability. This strategic addition significantly improved the exoskeleton’s overall performance.

### 5.1 Force control GUI

In developing the Force Control graphical user interface (GUI), our aim was to create a user-friendly platform for easy operation. The GUI comprises three main panels: ‘Force Sensor Threshold,’ ‘Exoskeleton Connection,’ and ‘Info’.

The ‘Force Sensor Threshold’ panel is crucial for configuring the control system, featuring sliders for inputting the ‘Upper Threshold’ and the ‘Lower Threshold,’ which serve as references for the system’s response.

Within the ‘Exoskeleton Connection’ sub-panel, users can select the COM port number linking their PC to the Exoskeleton’s microcontroller. They can also manually input the COM number if necessary. Successful connection initiation is indicated by a green ‘lamp’ within the GUI and a Yellow LED on the Exoskeleton.

The ‘Info’ panel provides real-time updates on various components, including the force sensor, threshold settings, and Exoskeleton battery status. It also includes a ‘Force

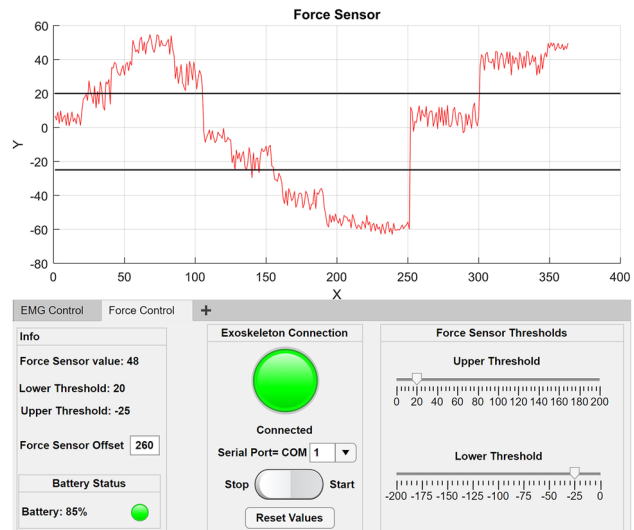


**Figure 9:** Force control graphical user interface allowing users to set and monitor two independent force thresholds for elbow flexion and elbow extension. The GUI enables real-time adjustment of the system’s response to muscle force, enhancing safety and usability.

Sensor Offset' edit field for adjusting the force sensor's reference point.

As seen in Figure 9, The GUI features a dynamic graph displaying filtered and unfiltered force sensor values, along with the upper and lower thresholds. This graphical representation offers users visual insight into the system's performance and control responses, facilitating real-time monitoring and adjustment of the exoskeleton's operation.

## 6 EMG control development

The Electromyogram (EMG) sensor is a part of the Classroom Exo system, as it detects and interprets electrical activity generated by muscle contractions, facilitated by conductive pads affixed to the skin. Each muscular contraction triggers electrical impulses within individual muscle fibers, leading to muscle activation.

In our setup, we utilize the Myoware Figure 10 Muscle Sensor as part of the EduExo Pro Kit provided by AUXIVO, purposefully designed for direct integration with a microcontroller. Unlike a raw EMG signal, this sensor's primary output is an amplified, rectified, and integrated signal, commonly referred to as the EMG envelope.

This processed signal is well-suited for interfacing with a microcontroller's analog-to-digital converter (ADC), enhancing its compatibility and functionality within our system. To illustrate this distinction, we provide a comparative representation of a typical EMG signal.

With a clear understanding of the EMG sensor's operation, we developed a simple yet efficient control system to respond to arm movements. Our system incorporates two Myo Ware Muscle Sensors, one on the bicep and the other on the triceps. The bicep sensor controls upward servo motion, while the triceps sensor manages downward motion [46], [47].

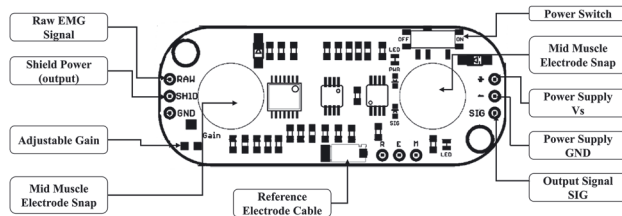


**Figure 10:** An overview of the Myo Ware Muscle Sensors' placement and connections, illustrating how these sensors detect muscle activity to control exoskeleton movements.

This setup is fundamental to our control system, which relies on two important thresholds: the 'Bicep Threshold' and the 'Triceps Threshold.' When the EMG sensor's output values surpass the 'Bicep Threshold,' the servo moves upward. Conversely, when the output values drop below the 'Triceps Threshold,' the servo moves downward. The servo's movement duration matches the applied force, ensuring a responsive system that adjusts to user actions.

### 6.1 EMG control GUI

In developing the EMG Control graphical user interface, our primary aim was to create an accessible and user-friendly platform for simplified operation. The GUI consists of three main panels: 'EMG Sensor Thresholds,' 'Exoskeleton Connection,' and 'Info.' The 'EMG Sensor Thresholds' panel is crucial for configuring the control system, housing sliders for user input of the 'Bicep Threshold' and 'Triceps Threshold,' serving as essential reference points for the system's responses (see Figure 11).

The 'Exoskeleton Connection' sub-panel integrates various components, with the 'Serial Port' drop-down field allowing users to designate the COM port number for connection. If the desired COM number is not listed, manual input is available. A successful connection is indicated by a green 'lamp' within the GUI and an Aqua LED on the

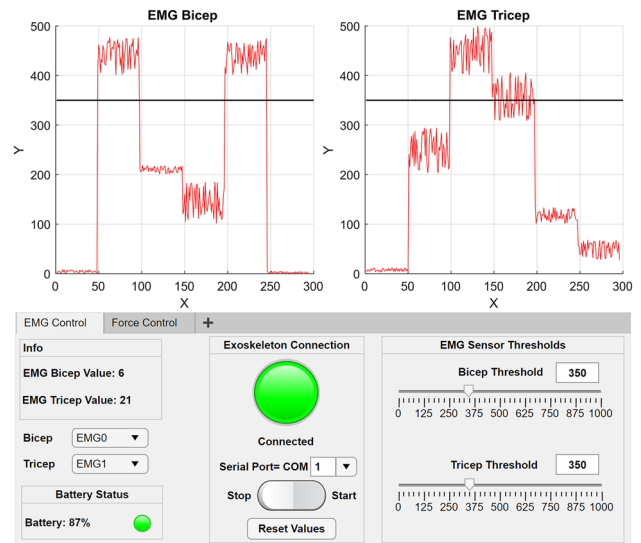


**Figure 11:** Electromyography (EMG) control graphical user interface featuring real-time monitoring of two muscle activities using Myo Ware Muscle Sensors. The GUI empowers users to set and adjust two independent thresholds, enabling seamless interaction and control.

Exoskeleton, with informative alerts provided for any connection issues.

The 'Info' panel serves as a dynamic repository of real-time information, updating users on EMG sensor data, threshold configurations, and the Exoskeleton's battery status. Drop-down fields allow users to designate the port to which each EMG sensor is connected, enhancing system adaptability.

The GUI features two graphs: one plotting Bicep EMG sensor values alongside its threshold, and another visualizing Triceps EMG sensor values with its threshold. These representations offer real-time insight into system performance, enabling users to monitor and fine-tune the Exoskeleton's operation.

## 7 Results

Throughout this development process, we have enhanced the functionality and usability of an exoskeleton system intended for educational use. Integration of advanced technologies and innovative solutions has led to significant improvements in its operation.

The exoskeleton is now utilized for teaching purposes in classroom and laboratory environments.

Key outcomes of this development include:

- Improved Power Management System: Upgrading from conventional AA batteries to a 2-cell Li-Polymer (LIPO) battery has increased the exoskeleton's power and a management system that allows regular charging with a USB cable, ensuring reliable operation even in demanding educational settings.
- Open-Source Educational Platform: Introducing the 'Classroom Exo,' an open-source educational robotic exoskeleton kit tailored for students and professionals in control engineering and biomedical engineering fields.
- Enhanced User Interface: The implementation of a user-friendly graphical interface with real-time feedback enables seamless monitoring and control of the exoskeleton, enhancing its accessibility for educational purposes.
- Threshold-Based Control: Implementation of threshold-based control systems enables responsive actions to user movements and applied forces, ensuring safe and efficient operation in conjunction with EMG and force sensors.

These advancements are depicted visually in Figure 12, providing a representation of The Classroom Exo.

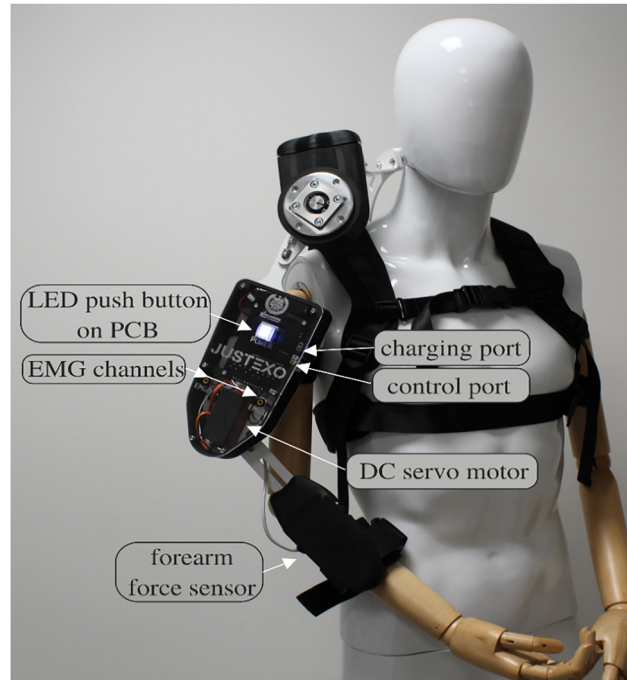


**Figure 12:** The Classroom Exo on a mannequin: The Classroom Exo has individual charging and control ports, 2 EMG channels, a forearm force sensor, and an LED push button for visual feedback to the user. A transparent cover allows users insights into the electronics.

## 8 Discussion

### 8.1 Upgrades for classroom readiness

To optimize the Classroom Exo for educational environments, several practical upgrades have been implemented to enhance usability and reliability. These include the design of a PCB with a protection system to safeguard the board and its components. Additionally, a charging USB port has been integrated for convenient battery recharging, ensuring smooth operation during classroom activities. The PCB design also allows for easy integration of additional sensors, enabling further experimentation and customization. LED feedback indicators have been added to provide visual cues to both students and instructors, offering real-time status updates during demonstrations. User-friendly graphical interfaces have been specifically tailored for classroom use, simplifying system operation and control.

With an open-access approach, the system encourages exploration and modification by students and educators, fostering collaborative learning experiences. Furthermore, comprehensive manuals and documentation are provided to ensure better utilization of the system and minimize disruptions in the classroom setting.

## 8.2 Educational concepts

The Classroom Exo system is designed to support a wide range of educational concepts and learning objectives. It can serve as a practical tool for teaching and learning in control theory and biomedical engineering fields. Through the Classroom Exo, students can gain hands-on experience with exoskeleton technology, deepening their understanding of its underlying principles.

The Classroom Exo allows students to engage with control theory concepts such as feedback control, proportional-integral (PI) controllers, and system stability. Through practical experimentation with the exoskeleton system, students can explore and observe how different controller parameters affect system behavior. Furthermore, the integration of graphical user interfaces facilitates intuitive interaction, enabling students to visualize control strategies and observe their impact in real-time.

Through the use of force sensors and EMG sensors, students can explore biomechanical concepts related to human movement, muscle activation, and interaction forces. This hands-on approach enhances understanding of biomechanical principles and their applications in assistive technologies and rehabilitation. Additionally, the platform's integration of threshold-based control mechanisms, EMG sensors, and force sensors introduces students to advanced concepts and practical applications, enhancing their academic learning and preparing them for potential careers in robotics and exoskeleton development.

## 9 Conclusions

Our work led to the development of the Classroom Exo, an open-source educational exoskeleton platform, which significantly enhances the usability and accessibility of exoskeleton technology for educators in the fields of control engineering and biomedical engineering. By improving the power source, power management, and providing intuitive user interfaces, we have created a classroom-ready versatile tool that empowers teachers and students to understand, experiment, and apply exoskeleton technology for various applications.

**Acknowledgment:** The authors want to thank Axel Sjögren-Holtz for his valuable support.

**Research ethics:** Not applicable.

**Author contributions:** The authors have accepted responsibility for the entire content of this manuscript and approved

its submission. M.T. and F.J. developed the educational exoskeletons and wrote the paper. B.L. and M.O.C. provided resources and feedback for the development. F.J. acquired the research funding.

**Competing interests:** The authors state no conflict of interest.

**Research funding:** The work was funded by the Solveig and Karl G. Eliasson Memorial Foundation, Nr. 9024012.

**Data availability:** The data is open access available <https://github.com/fabianjust/classroom-exo>.

## References

- [1] Y. H. Weng, C. H. Chen, and C. T. Sun, "Toward the human-robot co-existence society: on safety intelligence for next generation robots," *Int. J. Soc. Robot.*, vol. 1, no. 4, pp. 267–282, 2009.
- [2] E. Magrini, F. Ferraguti, A. J. Ronga, F. Pini, A. De Luca, and F. Leali, "Human-robot coexistence and interaction in open industrial cells," *Robot. Comput. Integr. Manuf.*, vol. 61, 2020, Art. no. 101846.
- [3] S. Zhang, S. Li, X. Li, Y. Xiong, and Z. Xie, "A human-robot dynamic fusion safety algorithm for collaborative operations of cobots," *J. Intell. Robot. Syst.: Theory Appl.*, vol. 104, no. 1, 2022, Art. no. 18.
- [4] A. Arslan, C. Cooper, Z. Khan, I. Golgeci, and I. Ali, "Artificial intelligence and human workers interaction at team level: a conceptual assessment of the challenges and potential HRM strategies," *Int. J. Manpow.*, vol. 43, no. 1, pp. 75–88, 2022.
- [5] A. Martinetti, P. K. Chemweno, K. Nizamis, and E. Fosch-Villaronga, "Redefining safety in light of human-robot interaction: a critical review of current standards and regulations," *Front. Chem. Eng.*, vol. 3, no. 666237, pp. 1–12, 2021.
- [6] W. Huo, S. Mohammed, J. C. Moreno, and Y. Amirat, "Lower limb wearable robots for assistance and rehabilitation: a state of the art," *IEEE Syst. J.*, vol. 10, no. 3, pp. 1068–1081, 2016.
- [7] Y. Zimmermann, *et al.*, "Human-robot attachment system for exoskeletons: design and performance analysis," *IEEE Trans. Robot.*, vol. 39, no. 4, pp. 3087–3105, 2023.
- [8] A. A. Morgan, J. Abdi, M. A. Q. Syed, G. El Kohen, P. Barlow, and M. P. Vizcaychipi, "Robots in healthcare: a scoping review," *Curr. Robot. Rep.*, vol. 3, no. 4, pp. 271–280, 2022.
- [9] M. Zhu, S. Biswas, S. I. Dinulescu, N. Kastor, E. W. Hawkes, and Y. Visell, "Soft, wearable robotics and haptics: technologies, trends, and emerging applications," *Proc. IEEE*, vol. 110, no. 2, pp. 246–272, 2022.
- [10] L. Morris, R. S. Diteesawat, N. Rahman, A. Turton, M. Cramp, and J. Rossiter, "The-state-of-the-art of soft robotics to assist mobility: a review of physiotherapist and patient identified limitations of current lower-limb exoskeletons and the potential soft-robotic solutions," *J. Neuroeng. Rehabil.*, vol. 20, no. 1, 2023, Art. no. 18.
- [11] A. Golabchi, A. Chao, and M. Tavakoli, "A systematic review of industrial exoskeletons for injury prevention: efficacy evaluation metrics, target tasks, and supported body postures," *Sensors*, vol. 22, no. 7, p. 2714, 2022.

- [12] Y. H. Ching, D. Yang, S. Wang, Y. Baek, S. Swanson, and B. Chittoori, "Elementary school student development of STEM attitudes and perceived learning in a STEM integrated robotics curriculum," *TechTrends*, vol. 63, no. 5, pp. 590–601, 2019.
- [13] K. Jaipal-Jamani and C. Angeli, "Effect of robotics on elementary preservice teachers' self-efficacy, science learning, and computational thinking," *J. Sci. Educ. Technol.*, vol. 26, no. 2, pp. 175–192, 2017.
- [14] H. Liu, J. Sheng, and L. Zhao, "Innovation of teaching tools during robot programming learning to promote middle school students' critical thinking," *Sustainability*, vol. 14, no. 11, p. 6625, 2022.
- [15] E. Afari and M. S. Khine, "Robotics as an educational tool: impact of lego mindstorms," *Int. J. Inf. Educ. Technol.*, vol. 7, no. 6, pp. 437–442, 2017.
- [16] B. Somuncu and D. Aslan, "Effect of coding activities on preschool children's mathematical reasoning skills," *Educ. Inf. Technol.*, vol. 27, no. 1, pp. 877–890, 2022.
- [17] T. Doleck, P. Bazelaïs, D. J. Lemay, A. Saxena, and R. B. Basnet, "Algorithmic thinking, cooperativity, creativity, critical thinking, and problem solving: exploring the relationship between computational thinking skills and academic performance," *J. Comput. Educ.*, vol. 4, no. 4, pp. 355–369, 2017.
- [18] B. Zhong and L. Xia, "A systematic review on exploring the potential of educational robotics in Mathematics education," *Int. J. Sci. Math. Educ.*, vol. 18, no. 1, pp. 79–101, 2020.
- [19] S. Blanchard, V. Freiman, and N. Lirrete-Pitre, "Strategies used by elementary schoolchildren solving robotics-based complex tasks: innovative potential of technology," in *Procedia – Social and Behavioral Sciences*, 2010, pp. 2851–2857.
- [20] G. Nugent, B. Barker, H. Lester, N. Grandgenett, and D. Valentine, "Wearable textiles to support student STEM learning and attitudes," *J. Sci. Educ. Technol.*, vol. 28, no. 5, pp. 470–479, 2019.
- [21] R. Ramos-Zúñiga and J. A. González-Rios, "The role of an exoskeleton simulation of senescence in health sciences education," *J. Environ. Public Health*, vol. 2023, no. 3148896, pp. 1–10, 2023.
- [22] D. Scaradozzi, L. Guasti, M. Di Stasio, B. Miotti, A. Monteriù, and P. Blikstein, "Makers at school, educational robotics and innovative learning environments," 2023, [Online]. Available at: <https://link.springer.com/bookseries/15179>.
- [23] J. Ortiz-Revilla, I. M. Greca, and I. Arriasecq, "A theoretical framework for integrated STEM education," *Sci. Educ.*, vol. 31, no. 2, pp. 383–404, 2022.
- [24] Y. Li, K. Wang, Y. Xiao, and J. E. Froyd, "Research and trends in STEM education: a systematic review of journal publications," *Int. J. STEM Educ.*, vol. 7, no. 1, 2020, Art. no. 11.
- [25] T. J. Kennedy and M. R. L. Odell, "STEM education as a meta-discipline," *SpringerLink*, vol. 56, pp. 37–51, 2023.
- [26] Y. Li, K. Wang, Y. Xiao, J. E. Froyd, and S. B. Nite, "Research and trends in STEM education: a systematic analysis of publicly funded projects," *Int. J. STEM Educ.*, vol. 7, no. 1, 2020, Art. no. 17.
- [27] Y. H. Ching and Y. C. Hsu, "Educational robotics for developing computational thinking in young learners: a systematic review," *TechTrends*, vol. 67, no. 3, pp. 1–12, 2023.
- [28] W. Luo, H. R. Wei, A. D. Ritzhaupt, A. C. Huggins-Manley, and C. Gardner-McCune, "Using the S-STEM survey to evaluate a middle school robotics learning environment: validity evidence in a different context," *J. Sci. Educ. Technol.*, vol. 28, no. 4, pp. 429–443, 2019.
- [29] P. Coufal, "Project-based STEM learning using educational robotics as the development of student problem-solving competence," *Mathematics*, vol. 10, no. 23, p. 4618, 2022.
- [30] A. Merkouris and K. Chorianopoulos, "Introducing computer programming to children through robotic and wearable devices," in *ACM International Conference Proceeding Series*, Association for Computing Machinery, 2015, pp. 69–72.
- [31] B. Barker, J. Melander, N. Grandgenett, and G. Nugent, "Utilizing wearable technologies as a pathway to STEM," in *Society for Information Technology & Teacher Education (SITE) conference proceedings*, 2015.
- [32] R. Bogue, "Exoskeletons: a review of recent progress," *Ind. Robot.*, vol. 49, no. 5, pp. 813–818, 2022.
- [33] R. Bogue, "Exoskeletons – a review of industrial applications," *Ind. Robot.*, vol. 45, no. 5, pp. 585–590, 2018.
- [34] F. Nazari, N. Mohajer, D. Nahavandi, A. Khosravi, and S. Nahavandi, "Applied exoskeleton technology: a comprehensive review of physical and cognitive human-robot interaction," *IEEE Trans. Cogn. Dev. Syst.*, vol. 15, no. 3, pp. 1102–1122, 2023.
- [35] R. Bogue, "Exoskeletons and robotic prosthetics: a review of recent developments," *Ind. Robot.*, vol. 36, no. 5, pp. 421–427, 2009.
- [36] S. O'Connor, "Exoskeletons in nursing and healthcare: a bionic future," *Clin. Nurs. Res.*, vol. 30, no. 8, pp. 1123–1126, 2021.
- [37] O. Atabek, D. C. C. Patricia, and A. E. Ertmer, "The challenges of integrating technology into education: a review of the literature," *J. Educ. Technol. Soc.*, vol. 13, no. 1, pp. 16–30, 2010.
- [38] R. J. Hartman, M. B. Townsend, and M. Jackson, "Educators' perceptions of technology integration into the classroom: a descriptive case study," *J. Res. Innov. Teach. Learn.*, vol. 12, no. 3, pp. 236–249, 2019.
- [39] C. Audrin and B. Audrin, "Key factors in digital literacy in learning and education: a systematic literature review using text mining," *Educ. Inf. Technol.*, vol. 27, no. 6, pp. 7395–7419, 2022.
- [40] R. Raja and P. C. Nagasubramani, "Recent trend of teaching methods in education" organised by sri sai bharath college of education dindigul-624710," *Indian J. Appl. Adv. Res.*, vol. 2018, no. 3, pp. 33–35, 2018.
- [41] K. A. Cintra, M. C. Borges, M. P. Panúncio-Pinto, L. E. de Almeida Troncon, and V. R. Bollela, "The impact and the challenges of implementing a faculty development program on health professions education in a Brazilian Medical School: a case study with mixed methods," *BMC Med. Educ.*, vol. 23, no. 1, 2023, Art. no. 784.
- [42] M. M. Rahman, et al., "Biomedical research in developing countries: opportunities, methods, and challenges," *Indian J. Gastroenterol.*, vol. 39, no. 3, pp. 292–302, 2020.

- [43] N. Teig, R. Scherer, and T. Nilsen, "I know I can, but do I have the time? The role of teachers' self-efficacy and perceived time constraints in implementing cognitive-activation strategies in science," *Front. Psychol.*, vol. 10, Jul. 2019, Art. no. 1697. <https://doi.org/10.3389/fpsyg.2019.01697>.
- [44] V. Bartenbach and C. Shirota, "Design and impact of a commercial educational robotic exoskeleton," *Biosyst. Biorobot.*, vol. 25, pp. 136–140, 2020.
- [45] B. Lennartson, *Reglerteknikens Grunder*, 4th ed. Gothenburg, Jens Fredholm, 2000, pp. 301–355.
- [46] L. Ajithkumar, P. Kumar, B. Vijaya Krishna, and P. Kumar, "Biomechanical aspects of muscle power analysis by using myoware muscle sensor," in *Proceedings – 2022 International Conference on Smart and Sustainable Technologies in Energy and Power Sectors, SSTEPS 2022*, Institute of Electrical and Electronics Engineers Inc., 2022, pp. 369–373.
- [47] H. Qassim, *et al.*, "Biceps and triceps electrical activity analysis based on using low-cost sensor: case study," in *International Workshop on Smart Info-Media Systems in Asia*, vol. 2022, no. SS1-4, pp. 15–20, 2022.

## Bionotes



### Mohammed Al-Tashi

Center of Bionics and Pain Research,  
Länsmansgatan 28, 431 30 Mölndal, Sweden  
[mohammedaltashi770@gmail.com](mailto:mohammedaltashi770@gmail.com)

Mohammed Al-Tashi is a mechatronic engineering working on health technologies and exoskeleton development at the Center for Bionics & Pain Research. Currently, he is a master student in mechatronics at Karabük University, Karabük, Turkey.



### Bengt Lennartson

Department of Electrical Engineering,  
Chalmers University of Technology,  
Chalmersplatsen 5, 42196, Gothenburg,  
Sweden  
[bengt.lennartson@chalmers.se](mailto:bengt.lennartson@chalmers.se)

Bengt Lennartson, Professor of Automation at Chalmers University of Technology since 1999, served as Associate Editor for *Automatica* and *IEEE Transaction on Automation Science and Engineering*. He chaired IEEE CASE 2015 and WODES 2008, and was Dean of Education at Chalmers. With 300+ peer-reviewed international papers, his current focus is AI planning, learning, and sustainable production. IEEE Fellow for contributions to hybrid systems for automation and sustainable production.



### Max Ortiz Catalan

Center of Bionics and Pain Research,  
Länsmansgatan 28, 431 30 Mölndal, Sweden;  
Bionics Institute, 384-388 Albert St, East  
Melbourne, VIC 3002, Australia; and Medical  
Bionics Department, University of Melbourne,  
Parkville VIC 3052, Australia  
[maxortizc@outlook.com](mailto:maxortizc@outlook.com)

Max Ortiz Catalán is the Head of Neural Prosthetic Research at the Bionics Institute and Honorary Principal Fellow at the University of Melbourne, both in Melbourne, Australia. He has authored over 100 scientific publications, and has been guest speaker in over 100 international conferences and universities worldwide. Several documentaries and over 100 popular science articles in over a dozen languages have featured his work, for which he has received several honors for innovation and scientific excellence.



**Fabian Just**

Center of Bionics and Pain Research,  
Länsmansgatan 28, 431 30 Mölndal, Sweden;  
and Department of Electrical Engineering,  
Chalmers University of Technology,  
Chalmersplatsen 5, 42196, Gothenburg,  
Sweden

**fabianjust@outlook.com**

**<https://orcid.org/0000-0002-9580-8189>**

Fabian Just is a postdoctoral researcher at the Center for Bionics & Pain Research in prosthetic control and neurotechnology development. He obtained a MSc in electrical engineering from Purdue University (IN, USA) in 2013 and a MSc in control engineering from Ruhr-University Bochum (Germany) in 2014. He finished his Ph.D. in rehabilitation robotics at ETH Zurich, Switzerland in 2020. As founding head-of-discipline, team manager, and advisory board member of the CYBATHLON, he fosters inclusion for people with disabilities.